Liver-specific deletion of negative regulator Pten results in fatty liver and insulin hypersensitivity

Bangyan Stiles*†, Ying Wang*, Andreas Stahl‡, Sara Bassilian§, W. Paul Lee§, Yoon-Jung Kim¶, Robert Sherwin¶, Sherin Devaskar‖, Ralf Lesche*,, Mark A. Magnuson††, and Hong Wu*†**

*Departments of Molecular and Medical Pharmacology and Howard Hughes Medical Institute and ‖Department of Pediatrics Neonatology and Developmental Biology, David Geffen School of Medicine, University of California, Los Angeles, CA 90095; ‡Research Institute, Palo Alto Medical Foundation and Stanford School of Medicine, Palo Alto, CA 94301; §Department of Pediatrics, Harbor-UCLA Medical Center, Los Angeles, CA 90502; ¶Department of Internal Medicine, Yale University School of Medicine, New Haven, CT 06520; and ††Department of Molecular Physiology and Biophysics, Vanderbilt University School of Medicine, Nashville, TN 37235

Communicated by Michael G. Rosenfeld, University of California at San Diego, La Jolla, CA, December 23, 2003 (received for review November 5, 2003)

In the liver, insulin controls both lipid and glucose metabolism through its cell surface receptor and intracellular mediators such as phosphatidylinositol 3-kinase and serine-threonine kinase AKT. The insulin signaling pathway is further modulated by protein tyrosine phosphatase or lipid phosphatase. Here, we investigated the function of phosphatase and tension homologue deleted on chromosome 10 (PTEN), a negative regulator of the phosphatidylinositol 3-kinase/AKT pathway, by targeted deletion of *Pten* in murine liver. Deletion of *Pten* in the liver resulted in increased fatty acid synthesis, accompanied by hepatomegaly and fatty liver phenotype. Interestingly, *Pten* liver-specific deletion causes enhanced liver insulin action with improved systemic glucose tolerance. Thus, deletion of *Pten* in the liver may provide a valuable model that permits the study of the metabolic actions of insulin signaling in the liver, and PTEN may be a promising target for therapeutic intervention for type 2 diabetes.

Insulin controls glucose and lipid homeostasis by modulating the function of multiple organs, including liver, muscle, and fat. In muscle and fat, insulin stimulates glucose uptake, resulting in glucose clearance from circulation. In liver, insulin promotes glycogen synthesis and glycolysis, as well as fatty acid (FA) synthesis. Impairment of the insulin signaling pathway plays a key role in the development of type 2 diabetes (T2D). Knockout and transgenic studies of molecules in this pathway have provided novel insights into the understanding of the molecular mechanisms underlying T2D (1). The muscle insulin receptor (IR) knockout model demonstrated normal insulin levels, in association with a metabolic syndrome characterized by defective FA metabolism (2). The liver IR knockout mice displayed severe insulin resistance and mild diabetes, in conjunction with hyperinsulinemia (3). Similar gene knockout studies were also performed with glucose transporter type-4 in muscle and fat (4, 5). Together with earlier studies (6) on murine models of obesity, these knockout studies revealed the importance of cooperation among different organs in the regulation of glucose and FA homeostasis (7), as well as the vital role liver plays in this collaboration.

The importance of phosphatidylinositol 3-kinase (PI3-kinase)/AKT in insulin signal has been suggested by both molecular and genetic studies (8–10). Insulin signal leads to the activation of PI3-kinase and its downstream target, AKT. One of the negative regulators of the insulin signaling pathway is PTEN (phosphatase and tension homologue deleted on chromosome 10), a lipid and protein phosphatase (11). In C-elegans, the PTEN homolog, DAF-18, acts in insulin receptor-like pathway and regulates longevity and dauer larva development (12–15). Hyperactivation of the PI3-kinase/AKT pathway also appears to be a main result of *Pten* deletion in mammalian systems (16). Unfortunately, *Pten*-deficient mice die at early stage of embryonic development (17–20), which precludes study of the role of PTEN in the mammalian insulin signaling pathway in a whole-animal setting. Injection of antisense oligonucleotide has demonstrated that inhibiting *Pten* may improve the glycemic control in *ob*/*ob* and *db*/*db* mice (21). In this study, we have generated an animal model by disrupting the *Pten* gene in mouse liver to assess the biological functions of PTEN in insulin signaling and the development of insulin resistance.

Materials and Methods

Animals. $Pten^{loxP/loxP}$ mice (22) were bred with Alb-Cre mice to generate mice with liver-specific deletion (23). All experiments were conducted in accordance with University of California, Los Angeles live animal welfare guidelines.

Animals 1, 3, and 6 months old were used for the experiments. For metabolic measurements, animals were fasted overnight. Blood samples were taken next morning for assessment of glucose, insulin (Linco and Alpco), nonesterified FAs (NEFA) (Wako), leptin (Crystal Chem) and triglyceride (TG) (Thermo DMA) by using manufactured kits. For tissue collection, mice were fasted overnight and blood was collected from cardiac puncture. Livers were perfused and collected in formalin for histology or in TRIzol (Invitrogen) for RNA. Extra liver tissues were flash-frozen in liquid nitrogen for protein analysis or frozen section.

Glucose Tolerance Test (GTT). A GTT was performed on mice that were fasted for 16 h. For glucose measurement, tail veins were punctured and a small amount of blood was released and applied onto a Therasense glucometer. For GTT, mice were given a single dose (2 g/kg of body weight) of D-dextrose (Sigma) by i.p. injection after a baseline glucose check. Circulating glucose levels were then measured at indicated time points after glucose injection.

Analysis of Long-Chain FA Uptake by Hepatocytes. Primary hepatocytes were prepared by two-step perfusion with liver perfusion and digestion medium, according to the manufacturer's instructions (Invitrogen), and were immediately used for uptake assays. Fluorescence-activated cell sorter-based short-term (30 sec) FA uptake assays were performed as described (24).

Analysis of FA Synthesis Rate By Using GC-MS. Deuterium water (D_2O; Aldrich) was provided as deuterium source for incorporation into the FA in *de novo* lipogenesis (25, 26). An initial priming dose of deuterium water (4% body weight) by i.p. injection was followed by a maintenance dose of 6% (vol/vol)

Abbreviations: FA, fatty acid; NEFA, nonesterified FA; T2D, type 2 diabetes; PI3-kinase, phosphatidylinositol 3-kinase; PTEN, phosphatase and tension homologue deleted on chromosome 10; TG, triglyceride; GTT, glucose tolerance test; PTP, protein tyrosine phosphatase; GS, glycogen synthase; PEPCK, phospho*enol*pyruvate carboxykinase; G6Pase, glucose-6-phosphatase.

†To whom correspondence may be addressed. E-mail: bstiles@mednet.ucla.edu or hwu@mednet.ucla.edu.

**Present address: Epigenomics AG, Kastanienallee 24, 10435 Berlin, Germany.

www.pnas.org/cgi/doi/10.1073/pnas.0308617100

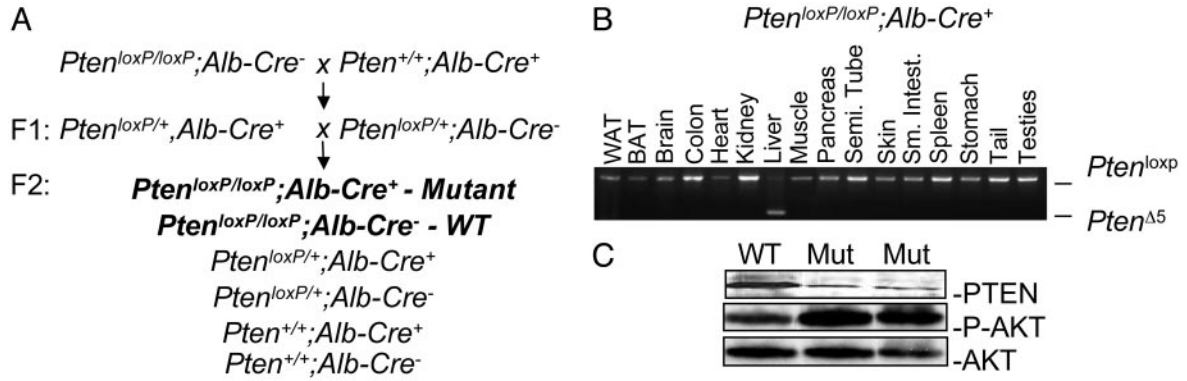

Fig. 1. Liver-specific deletion of *Pten*. (*A*) Breeding strategy. (*B*) Liver-specific deletion of the *Pten* gene. PCR analysis of DNA from different tissues of $Pten^{lox/lox}$;*Alb-Cre*$^{+}$ mice. (*C*) Western analysis for PTEN (*Top*), *p*-AKT (*Middle*) and AKT (*Bottom*).

D_2O in drinking water. Plasma samples were collected from orbital eye bleeding before and at 2, 4, 7, and 9 days after D_2O injection. At the end of the experiment, tissue samples were collected from perfused livers after overnight fasting. Total lipid was isolated from both plasma and liver samples after saponification. The isolated FAs were methylated and injected onto GC/MS with C-18 column. The spectrum of the palmitate peak (270–276 m/z) was analyzed for its isotopomer distribution and deuterium content, which were used to calculate the fraction of newly synthesized FA (25, 26).

Assessment of Lipid Secretion Rate *in Vivo*. Overnight-fasted mice were injected with 10% tyloxapol (5 μl/g body weight) through the tail vein to coat the lipoprotein particles. Plasma was collected through orbital eye bleeding before and 30, 60, and 90 min after tyloxapol injection, and TG levels were determined (27).

Western Blot Analysis. Liver samples were homogenized in PBS (pH 74)/1% NP-40/0.5% sodium deoxycholate/0.1% SDS containing protease inhibitors. For SDS/PAGE, 50 μg of protein was loaded. Blots were probed with PTEN, phospho-AKT, AKT, phospho-GSK-3 (Cell Signaling Technology, Beverly, MA), and FA synthase (FAS) from BD Bioscience. Same membranes (Bio-Rad) were also probed with actin or vinculin (Sigma) for loading controls.

Northern Blot Analysis. RNA samples were extracted from fresh liver by using TRIzol reagents. For RNA blot, 10 μg of RNA per sample was loaded. Blots were probed with phospho*enol*pyruvate carboxykinase (PEPCK), glucose-6-phosphatase (G6Pase), and actin for loading control. Probes for PEPCK and G6Pase are generous gifts from E. G. Beale (Texas Tech University, Lubbock, TX) and K. Van Auken (University of Colorado, Denver), respectively.

Statistical Analysis. All data are subjected to statistical analysis by using the EXCEL DATA ANALYSIS TOOL PAK (Microsoft). A Student's t test was used to determine the differences between the WT and mutant groups. A P value of 0.05 or less was considered significant.

Results

Liver-Specific *Pten* Deletion. We crossed $Pten^{loxP/loxP}$ mice with hepatocyte specific Alb-Cre-transgenic (23) mice to achieve liver-specific *Pten* deletion. The breeding strategy is illustrated in Fig. 1*A*. To avoid potential variations contributed by gender and genetic background, male mice from the F_2 generation, $Pten^{loxp/loxp}$;*Alb-Cre*$^{+}$ (mutant) and $Pten^{loxp/loxp}$;*Alb-Cre*$^{-}$ (WT), were used for studies described below. PCR analysis of $Pten^{loxp/loxp}$;*Alb-Cre*$^{+}$ mice showed that *Pten* deletion, as indicated by excision of the *Pten* locus ($Pten^{\Delta 5}$), is specific to liver with no leakage to other tissues, including white and brown adipose tissues (Fig. 1*B*), which is consistent with the previous report (23). As a result of *Pten* deletion, we observed hyperphosphorylation of AKT in the mutant livers (Fig. 1*C*; P-AKT). A Residual amount of PTEN observed in mutant livers was possibly contributed by cell types other than hepatocytes (Fig. 1*C* and ref. 23).

***Pten* Deletion in the Liver Results in Hepatomegaly, Fatty Liver, and Increased Glycogen Synthesis.** Examination of the mutant liver revealed pale color and marked hepatomegaly (Fig. 2*A Left Upper*). Concomitant with increased liver size, the liver weight and the ratio of liver weight to body weight in the mutant animals were also significantly increased (Fig. 2*A Lower*, $P \leq 0.05$). Histological analysis demonstrated significant morphological changes of mutant livers. The mutant hepatocytes were distended by large cytoplasmic vacuoles that push the nucleus against the cell membrane (Fig. 2*B*, arrows in *Top Right*), although the general lobular architecture remained. Because AKT activation could increase glycogen synthesis as well as FA synthesis, we stained liver sections with periodic acid Schiff's to visualize glycogen, and Oil red O for FAs. Staining with periodic acid Schiff's demonstrated increased glycogen storage in the mutant livers (Fig. 2*B Middle Right*). Strikingly, significant lipid deposition, as indicated by Oil red O staining, was observed in the mutant livers but not in age- and genetic background-matched WT mice (Fig. 2*B Bottom Right*). Quantification of liver TG content revealed a 3-fold increase in the mutant liver (Fig. 2*A Right Lower*), further confirming the fatty liver phenotype.

The progression of fatty liver phenotype appeared to be age-dependent. At 1 month of age, the mutant hepatocytes appeared swollen with minimal lipid deposition, starting from the area surrounding the central terminal hepatic venule (Fig. 1*A Top*). By 3 months of age, a substantial amount of lipid accumulation in the mutant hepatocytes was clearly evident, which further progress to entire liver by 6 months (Fig. 7, which is published as supporting information on the PNAS web site). Infiltration of inflammatory cells and mild fibrosis were observed in some but not all mutant livers at 6 months of age (data not shown). No apparent histological changes were observed in other tissues.

***Pten* Deletion Enhances the FA Synthesis in the Mutant Liver.** To understand the mechanisms underlying liver steatosis, we investigated the sources of lipid in the mutant hepatocytes. Accumulation of fat in the liver could be multifactorial, including increased uptake from peripheral and/or enhanced *de novo* FA

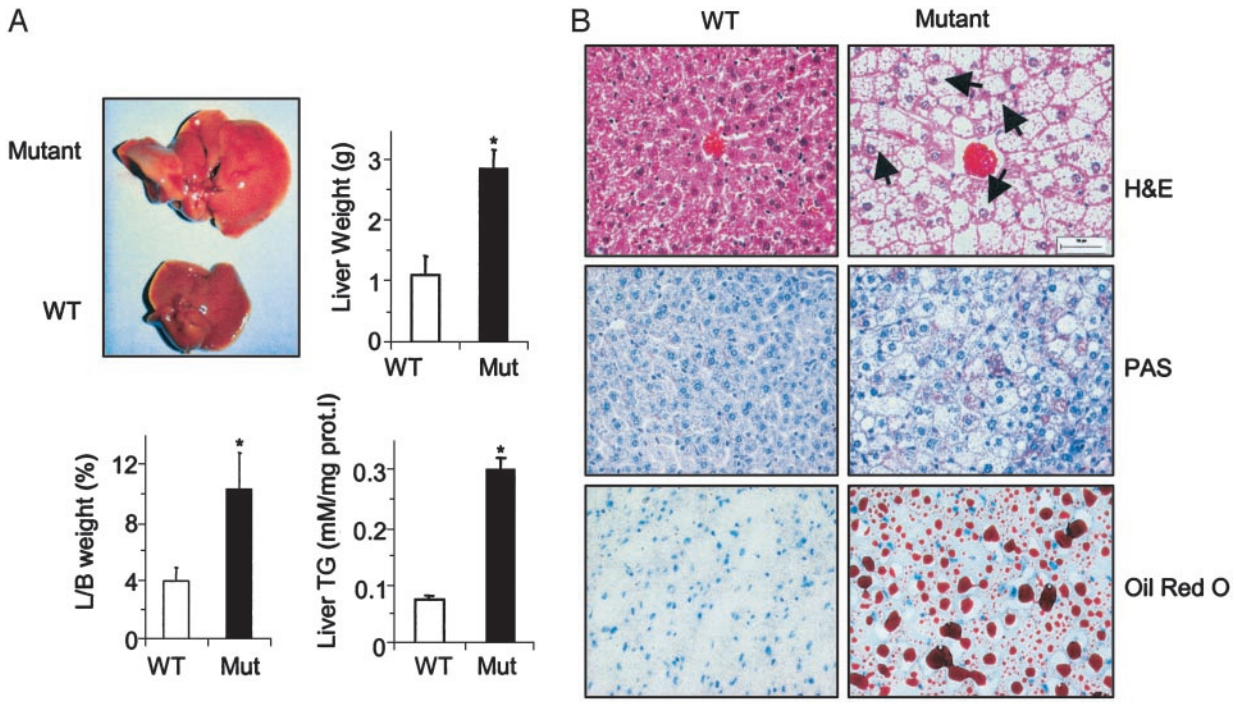

Fig. 2. *Pten* deletion results in hepatomegaly and liver steatosis. (*A*) Hepatomegaly of mutant mice. Photo shows livers from mutant (*Upper*) and WT mouse (*Lower*); mutant mice have heavier livers (*Upper Right*; $n = 6$), increased liver to body weight ratio (*Lower Left*; $n = 6$), and increased TG storage (*Lower Right*; $n = 6$). *, $P \leq 0.05$. (*B*) Histological analysis of liver sections from WT and mutant mice. (*Top*) Hematoxylin/eosin staining. (*Middle*) Periodic acid Schiff's staining (*Bottom*) Oil red O staining. (Bar, 50 μM.)

synthesis by the hepatocytes. We first investigated whether PTEN loss may cause increased FA uptake by isolating primary hepatocytes from 3-month-old WT and mutant mice and examining FA uptake by using fluorescent labeled long-chain FA analogue and fluorescence-activated cell sorter analysis. FAs enter hepatocytes through either passive diffusion (low uptake) or active transportation (high uptake) (28), which can be easily separated by fluorescence-activated cell sorter analysis (24). In WT livers, ≈80% of the hepatocytes are in the low-uptake group. However, the mean uptake of the entire hepatocyte population depends on the high-uptake group because their uptake rates are two orders of magnitude higher than that of the low-uptake group (24). In mutant hepatocytes, uptake by the low-uptake group was significantly increased by 20%, whereas no significant difference was observed in the high-uptake group (Fig. 3*A*). As a net result, total FA uptake by the mutant hepatocytes was not significantly altered. This result was further supported by measuring the levels of two major liver FA transports, FATP2 and FATP5 (28). No significant differences were observed in the protein levels of these two transporters (data not shown).

Increased *de novo* lipogenesis is the other way in which FA can accumulate in the liver. To separate the direct effect of PTEN on FA synthesis from accumulated pathological effects of liver steatosis in aged animals, only 1-month-old male mice were used. We measured the rate of *de novo* FA synthesis by using D_2O and GC/MS (25, 26). Deuterium incorporation into newly synthesized FAs provides a sensitive measurement for the rate of *de novo* lipogenesis. We demonstrated that the rate of FA synthesis is 2.5-fold higher in the mutant livers (Fig. 3*B Left*, $P \leq 0.05$), as compared with the WT livers. To assess whether the newly synthesized FAs could be released to plasma, we measured lipid secretion rate by injecting triton. Lipid output by hepatocytes is mediated by lipoproteins that complex with various lipid molecules to form lipolipoprotein particles. Triton coats these lipid particles (27) and inhibits their peripheral absorption. The plasma TG levels in the mutant mice were higher than that of the WT mice at every time point measured after triton injection (Fig. 3*B Right*; $P \leq 0.05$), suggesting that *Pten* deletion leads to higher rates of both FA synthesis and secretion.

Liver Steatosis Is Accompanied by Decreased Body Fat Content. As a result of *Pten* deletion in the liver, we also observed a 50% reduction of total body fat content (Fig. 3*C Left Upper*) as measured with NMR (29). Consistent with this sensitive *in vivo* measurement, the mutant animals at 1 month of age also showed decreased serum leptin levels (Fig. 3*C Left Lower*). No changes in feeding behavior, as measured by daily food intake, was observed that could account for the declined leptin in mutant mice, because animals from either group consumed 3 ± 0.5 g per animal per day. Interestingly, despite normal levels of plasma TG in the mutant animals (Fig. 3*C Right Lower*), there is a 30% decrease in circulating free FAs (NEFA) levels (Fig. 3*C Right Upper*), which is most likely due to decreased lipolysis rate, as measured by the *in vivo* lipolysis assay (Fig. 8, which is published as supporting information on the PNAS web site). Taken together, these results suggest that *Pten* liver-specific deletion may lead to redistribution of fat from other tissues to the liver.

Liver-Specific Deletion of *Pten* Causes Decreased Fasting Glucose Levels and Improved Glucose Tolerance. Because the levels of NEFA are thought to have a significant influence on insulin sensitivity, we measured both basal glucose levels and the rates of glucose clearance on animals at 1, 3, and 6 months of age. Deleting *Pten* caused a decrement in fasting plasma glucose levels in 1- and 3-month-old mice (Fig. 4*A Left* and *Center*, $P \leq 0.05$). This occurrence of lowered glucose concentration was accompanied by a significant decrease in fasting plasma insulin levels (Fig. 4*B Left*). At 6 months of age, when severe steatosis was observed in the liver, the fasting glucose level in the mutant

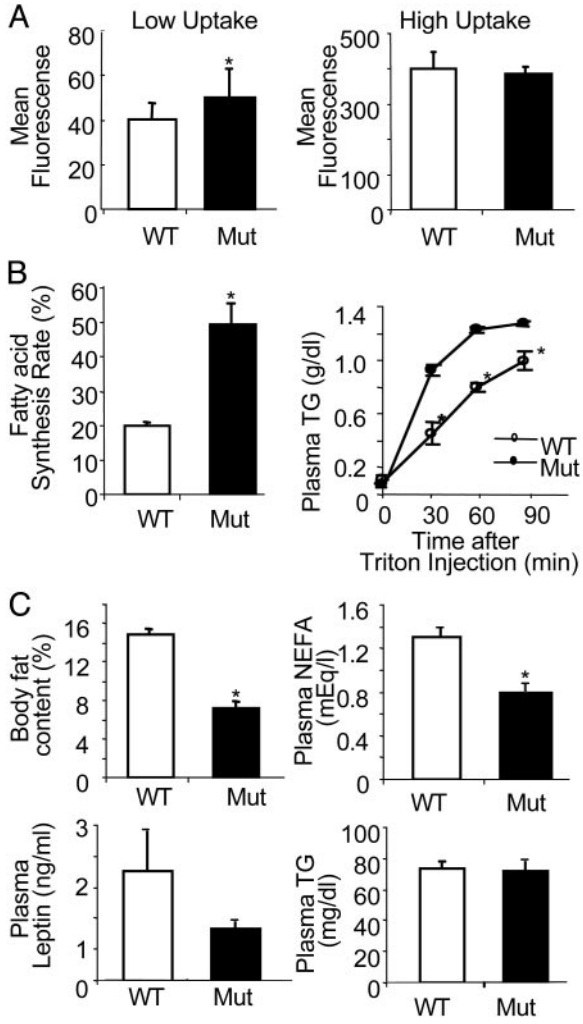

Fig. 3. *Pten* deletion enhances FA synthesis and secretion by hepatocytes. (*A*) Uptake of long-chain FA by WT and mutant primary hepatocytes. (*Left*) Low-uptake group. (*Right*) High-uptake group. $n = 3$. (*B*) FA synthesis rate is calculated as newly synthesized portion of palmitate (*Left*, $n = 6$). Lipid secretion rate is measured as plasma TG levels at indicated time points after triton injection (*Right*, $n = 3$). (*C*) Lipid indexes of 1-month-old *Pten* WT and mutant mice: (*Left Upper*) body fat content of WT ($n = 7$) and mutant mice ($n = 6$). (*Right Upper*) Plasma NEFA levels in WT ($n = 6$) and mutant ($n = 6$) mice. (*Left Lower*) Plasma leptin levels in WT ($n = 5$) and mutant mice ($n = 5$). (*Right Lower*) Plasma TG levels in WT ($n = 5$) and mutant mice ($n = 5$). *, $P \leq 0.05$.

mice was comparable with that of the WT mice (Fig. 4*A Right*), suggesting that even though the insulin level in the mutant remained lower than WT mice (Fig. 4*B Right*), accumulated liver damage has started to influence liver function.

When challenged with an i.p. glucose load, the mutant mice demonstrated a lower peak glucose concentration at 15 min (by 30%, $P \leq 0.05$) and a faster decline of plasma glucose levels throughout the glucose tolerance curve (Fig. 5*A*, $P \leq 0.05$). The increased glucose clearance during an i.p. glucose load occurred in all age groups in mutant mice (Fig. 5) but is most evident in mice at 1 month of age: plasma glucose levels in mutants returned to baseline between 60 and 120 min, whereas it remained above baseline at 120 min in WT animals. These results suggest that *Pten* deletion in the liver not only causes increased insulin action in the liver, as indicated by increased glycogen and FA deposition, but also enhances glucose disposal.

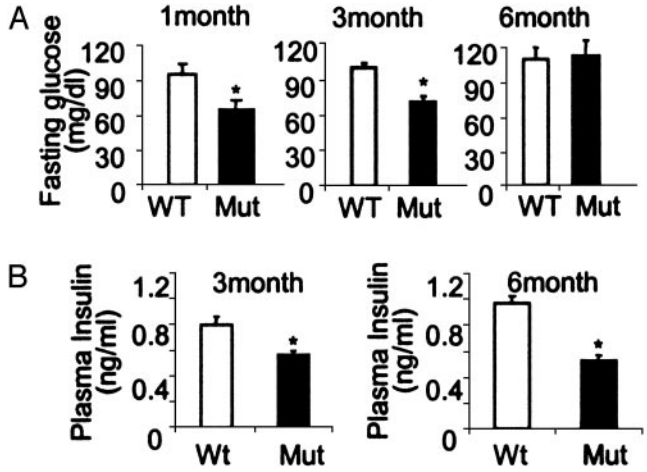

Fig. 4. Fasting plasma glucose and insulin levels. (*A*) Fasting plasma glucose levels in 1- (*Left*), 3- (*Center*), and 6-month-old (*Right*) mice. Open bars, WT ($n = 9$); filled bars, mutant ($n = 11$). (*B*) Fasting plasma insulin concentrations in 3- (*Left*) and 6-month-old (*Right*) mice. $n = 6$. *, $P \leq 0.05$.

***Pten* Regulates Key Enzymes Controlling Glycogen and FA Syntheses.** To correlate between the metabolic phenotypes and alterations of insulin-controlled signaling pathway in mutant liver, we investigated the expression of a number of genes involved in glucose and lipid metabolism. GSK-3 is the key molecule negatively regulating glycogen synthase (GS), which is required for the incorporation of glucose into glycogen. GSK-3 constitutively phosphorylates GS to inactive its enzymatic activity. Phosphorylation of GSK-3 by AKT inactivates the kinase and relieves its block on GS (30). We showed that phosphorylation of GSK-3β was moderately increased (50%) when *Pten* is deleted (Fig. 6*A*). Thus, GSK-3β hyperphosphorylation may account for the increased glycogen accumulation observed in mutant livers. Deletion of *Pten* resulted in a marked increase in liver FAS levels (Fig. 6*A*), which is likely to play an important role in the increased *de novo* FA synthesis observed in the mutant livers. In contrast, there was down-regulation of two key gluconeogenic enzymes in the mutant mice, namely glucose-6-phosphatase (G6Pase) and PEPCK. The expression of these two enzymes was similarly decreased in the mutant livers although the change in PEPCK was more pronounced (Fig. 6*B*). Together, the changes in FAS, G6Pase, and PEPCK enzyme levels may divert substrate toward FA synthesis.

Discussion

Because T2D is characterized by an impaired insulin action, research efforts have focused on understanding the insulin-

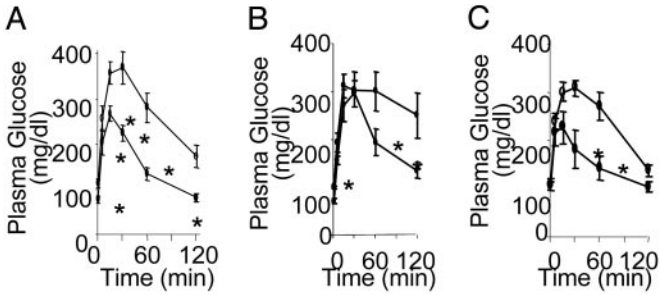

Fig. 5. i.p. GTT. (*A*) One-month GTT with WT ($n = 9$) and mutant ($n = 11$) mice. (*B*) Three-month GTT with WT ($n = 6$) and mutant ($n = 8$) mice. (*C*) Six-month GTT with WT ($n = 11$) and mutant ($n = 8$) mice. *, $P \leq 0.05$

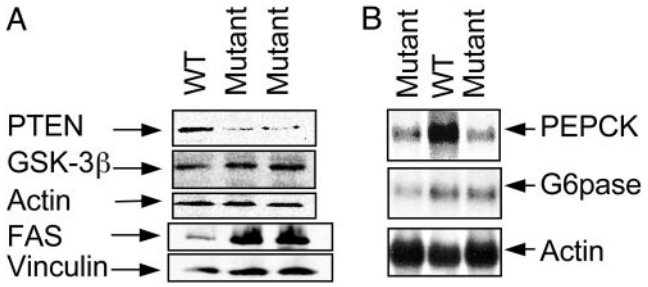

Fig. 6. *Pten* deletion results in inhibition of gluconeogenesis and activation of lipogenesis enzymes in the liver. (*A*) Western blot analysis of GSK-3β and FAS. Blots were probed with PTEN (first section), phospho-GSK-3β (second section), and FAS (fourth section). Actin and vinculin were used as loading controls. (*B*) Northern blot analysis of PEPCK and G6Pase gene expressions in mouse liver. Actin was used as loading control.

signaling pathway in an attempt to identify suitable therapeutic target(s) for drug intervention. Although significant progress has been made in the understanding of insulin activation, less is known about the negative control mechanisms that result in returning the activated IR to basal level. Because IR has intrinsic tyrosine kinase activity, various protein tyrosine phosphatases (PTPs) have been studied and implicated in controlling insulin receptor dephosphorylation and inactivation (31). In this study, we provided evidence that PTEN, a lipid phosphatase, serves as an important negative modulator for the insulin-signaling pathway by antagonizing the PI3-kinase/AKT signaling pathway. Thus, the role of PTEN in regulating insulin signaling pathway is evolutionary conserved from *Caenorhabditis elegans* (12) to mammals.

Deletion of *Pten* in the liver led to increased insulin sensitivity in the liver and improved overall glucose tolerance. Not surprisingly, the *Pten* liver deletion mouse shares similarity to PTP-1B knockout mouse. PTP-1B is a tyrosine phosphatase that negatively regulates IR signaling by presumably dephosphorylating IR, IRSs, or possibly other phosphotyrosyl molecules in the insulin-signaling pathway. PTP-1B deficiency causes insulin sensitivity, as demonstrated by lower glucose levels and improved glucose clearance in an i.p. glucose load (32), similar to what we observed in the liver-specific *Pten* deletion mouse. In contrast, phenotype associated with *Pten* liver-specific deletion is completely opposite to the insulin-resistant phenotype observed in the liver IR knockout mouse, which consists of severe liver insulin resistance and mild diabetes with hyperinsulinemia (3). Thus, our study provide, to our knowledge, the first genetic evidence for the role of PTEN in controlling the insulin-signal pathway in mammals *in vivo* and suggests that perturbing the functions of the negative regulators of the insulin-signaling pathway, either at the receptor level, as PTP-1B for IR, or on its downstream mediators, as PTEN for PI3-kinase/AKT, may lead to increased insulin sensitivity.

Lipid metabolism is also affected in *Pten* mutant mice. Similar to PTP-1B mice, which have increased energy expenditure and decreased adiposity (33), the *Pten* liver-specific deletion mice have decreased total body fat, and serum NEFA and leptin levels. Whether PTEN liver deficiency will lead to increase energy expenditure and resistance to diet-induced obesity, as reported for PTP-1B$^{-/-}$ mice, remains to be investigated. Furthermore, it is not clear whether lean body mass and hepatosteatosis in *Pten* mutant mice may alter the production and signaling of adiponectin, an adipocyte hormone involved in whole-body energy expenditure (34–36).

Unlike the PTP-1 knockout mouse, deleting *Pten* in the liver led to the development of hepatomegaly and fatty liver. Fatty liver has also been observed in *ob/ob* mice, a type II diabetes model (37, 38). Several fatty liver (nonalcoholic fatty liver disease) models exist, including the *fa/fa* rats and the lipoatrophic mice (39–41). The common denominator for these fatty liver models is hyperinsulinemic and insulin resistance, despite the differences in plasma leptin level and adipose tissue mass. In humans, liver steatosis is known to associate with obesity and diabetes conditions with hyperinsulinemia and insulin resistance (42). It was postulated that the high level of NEFA in circulation due to peripheral insulin resistance is the primary cause of fatty liver (43, 44). We showed in *Pten* mutants, a different fatty liver phenotype from that of hyperinsulinemic and insulin-resistant models. Fatty liver in our *Pten* mutant is associated with relative hypoinsulinemia, enhanced insulin action and low plasma NEFA, which is concomitant with lipoatrophy. Thus, our model has provided an insight into the mechanisms responsible for liver steatosis.

Recent studies (45–47) also suggest that the interaction among the different insulin-sensitive organs may be mediated through interactions between insulin and leptin signaling pathways, which may converge onto AKT and its effectors, such as the forkhead transcription factors and other not-yet-identified targets (48). In the *ob/ob* or knockout models, insulin resistance accompanies defects in leptin action in the liver (2–4, 38, 41, 47). *In vivo*, PTP-1B regulates leptin signal transduction, likely by targeting Jak2 (49). Interestingly, in the *Pten* liver knockout, increased insulin sensitivity is accompanied by hypoleptinemia.

The interplay between glucose and lipid metabolism is mediated by the reciprocal relationship of substrate use and distribution between liver and peripheral tissues. This relationship was observed in the IR/glucose transporter knockout mice with decreased glucose utilization (2, 4, 50), or in the *ob/ob* model with increased lipogenesis (38). In our study, the hepatosteatosis phenotype was accompanied by improved glucose tolerance and leaner body mass in mutant mice. In this case, enhanced insulin signaling in the liver resulted in redistribution of body fat from fatty tissue to the liver. The liver also appeared to be using more glucose for lipogenesis, as evidenced by the reduced levels of gluconeogenic enzymes. As a result, liver consumes more energy to synthesize and store fat. Thus, liver became the sacrificial organ to maintain glucose control and lean body mass.

In summary, we have created a valuable model for studying insulin action in the liver, as well as the complex interaction among insulin-sensitive organs and the reciprocal regulations of glucose and lipid metabolisms. The similarities shared by *Pten*-deficient mice and PTP-1B$^{-/-}$ mice further emphasize the importance of the negative regulators in normal insulin signaling and in the development of T2D and suggest that PTEN may be an attractive candidate or target for inhibitors as therapeutic intervention in the treatment of T2D.

We thank Dr. Kurlawalla and Dr. Wong for reading the manuscript and Gopel Sundaresan, Jun Wu, and Brian Blavo for technical support. H.W. is an Assistant Investigator of the Howard Hughes Medical Institute and a V Foundation Scholar. This work was partially supported by Department of Defense Grants DAMD17-00-1-0010 (to B.S.) and PC991538, National Institutes of Health Grants DK56339 (to A.S.) and CA98013, and CapCure (to H.W.).

1. Baudry, A., Leroux, L., Jackerott, M. & Joshi, R. L. (2002) *EMBO Rep.* **3,** 323–328.
2. Bruning, J. C., Michael, M. D., Winnay, J. N., Hayashi, T., Horsch, D., Accili, D., Goodyear, L. J. & Kahn, C. R. (1998) *Mol. Cell* **2,** 559–569.
3. Michael, M. D., Kulkarni, R. N., Postic, C., Previs, S. F., Shulman, G. I., Magnuson, M. A. & Kahn, C. R. (2000) *Mol. Cell* **6,** 87–97.
4. Abel, E. D., Peroni, O., Kim, J. K., Kim, Y. B., Boss, O., Hadro, E., Minnemann, T., Shulman, G. I. & Kahn, B. B. (2001) *Nature* **409,** 729–733.
5. Zisman, A., Peroni, O. D., Abel, E. D., Michael, M. D., Mauvais-Jarvis, F., Lowell, B. B., Wojtaszewski, J. F., Hirshman, M. F., Virkamaki, A., Goodyear, L. J., *et al.* (2000) *Nat. Med.* **6,** 924–928.

6. Koteish, A. & Mae Diehl, A. (2002) *Best Pract. Res. Clin. Gastroenterol.* **16,** 679–690.
7. Accili, D., Kido, Y., Nakae, J., Lauro, D. & Park, B. C. (2001) *Curr. Mol. Med.* **1,** 9–23.
8. Huisamen, B., van Zyl, M., Keyser, A. & Lochner, A. (2001) *Mol. Cell. Biochem.* **223,** 15–25.
9. Nakae, J., Kitamura, T., Silver, D. L. & Accili, D. (2001) *J. Clin. Invest.* **108,** 1359–1367.
10. Cho, H., Mu, J., Kim, J. K., Thorvaldsen, J. L., Chu, Q., Crenshaw, E. B., III, Kaestner, K. H., Bartolomei, M. S., Shulman, G. I. & Birnbaum, M. J. (2001) *Science* **292,** 1728–1731.
11. Sun, H., Lesche, R., Li, D. M., Liliental, J., Zhang, H., Gao, J., Gavrilova, N., Mueller, B., Liu, X. & Wu, H. (1999) *Proc. Natl. Acad. Sci. USA* **96,** 6199–6204.
12. Ogg, S. & Ruvkun, G. (1998) *Mol. Cell* **2,** 887–893.
13. Mihaylova, V. T., Borland, C. Z., Manjarrez, L., Stern, M. J. & Sun, H. (1999) *Proc. Natl. Acad. Sci. USA* **96,** 7427–7432.
14. Rouault, J. P., Kuwabara, P. E., Sinilnikova, O. M., Duret, L., Thierry-Mieg, D. & Billaud, M. (1999) *Curr. Biol.* **9,** 329–332.
15. Gil, E. B., Malone Link, E., Liu, L. X., Johnson, C. D. & Lees, J. A. (1999) *Proc. Natl. Acad. Sci. USA* **96,** 2925–2930.
16. Stiles, B., Gilman, V., Khanzenzon, N., Lesche, R., Li, A., Qiao, R., Liu, X. & Wu, H. (2002) *Mol. Cell. Biol.* **22,** 3842–3851.
17. Stambolic, V., Suzuki, A., de la Pompa, J. L., Brothers, G. M., Mirtsos, C., Sasaki, T., Ruland, J., Penninger, J. M., Siderovski, D. P. & Mak, T. W. (1998) *Cell* **95,** 29–39.
18. Di Cristofano, A., Pesce, B., Cordon-Cardo, C. & Pandolfi, P. P. (1998) *Nat. Genet.* **19,** 348–355.
19. Suzuki, A., de la Pompa, J. L., Stambolic, V., Elia, A. J., Sasaki, T., del Barco Barrantes, I., Ho, A., Wakeham, A., Itie, A., Khoo, W., *et al.* (1998) *Curr. Biol.* **8,** 1169–1178.
20. Podsypanina, K., Ellenson, L. H., Nemes, A., Gu, J., Tamura, M., Yamada, K. M., Cordon-Cardo, C., Catoretti, G., Fisher, P. E. & Parsons, R. (1999) *Proc. Natl. Acad. Sci. USA* **96,** 1563–1568.
21. Butler, M., McKay, R. A., Popoff, I. J., Gaarde, W. A., Witchell, D., Murray, S. F., Dean, N. M., Bhanot, S. & Monia, B. P. (2002) *Diabetes* **51,** 1028–1034.
22. Lesche, R., Groszer, M., Gao, J., Wang, Y., Messing, A., Sun, H., Liu, X. & Wu, H. (2002) *Genesis* **32,** 148–149.
23. Postic, C. & Magnuson, M. A. (2000) *Genesis* **26,** 149–150.
24. Stahl, A., Hirsch, D. J., Gimeno, R. E., Punreddy, S., Ge, P., Watson, N., Patel, S., Kotler, M., Raimondi, A., Tartaglia, L. A. & Lodish, H. F. (1999) *Mol. Cell* **4,** 299–308.
25. Lee, W. N., Bassilian, S., Guo, Z., Schoeller, D., Edmond, J., Bergner, E. A. & Byerley, L. O. (1994) *Am. J. Physiol.* **266,** E372–E383.
26. Lee, W. N., Bassilian, S., Lim, S. & Boros, L. G. (2000) *Am. J. Physiol.* **279,** E425–E432.
27. Li, X., Catalina, F., Grundy, S. M. & Patel, S. (1996) *J. Lipid Res.* **37,** 210–220.
28. Stahl, A., Gimeno, R. E., Tartaglia, L. A. & Lodish, H. F. (2001) *Trends Endocrinol. Metab.* **12,** 266–273.
29. Barac-Nieto, M. & Gupta, R. K. (1996) *J. Magn. Reson. Imaging* **6,** 235–238.
30. Cross, D. A., Alessi, D. R., Cohen, P., Andjelkovich, M. & Hemmings, B. A. (1995) *Nature* **378,** 785–789.
31. Asante-Appiah, E. & Kennedy, B. P. (2003) *Am. J. Physiol.* **284,** E663–E670.
32. Elchebly, M., Payette, P., Michaliszyn, E., Cromlish, W., Collins, S., Loy, A. L., Normandin, D., Cheng, A., Himms-Hagen, J., Chan, C. C., *et al.* (1999) *Science* **283,** 1544–1548.
33. Klaman, L. D., Boss, O., Peroni, O. D., Kim, J. K., Martino, J. L., Zabolotny, J. M., Moghal, N., Lubkin, M., Kim, Y. B., Sharpe, A. H., *et al.* (2000) *Mol. Cell. Biol.* **20,** 5479–5489.
34. Arita, Y., Kihara, S., Ouchi, N., Takahashi, M., Maeda, K., Miyagawa, J., Hotta, K., Shimomura, I., Nakamura, T., Miyaoka, K., *et al.* (1999) *Biochem. Biophys. Res. Commun.* **257,** 79–83.
35. Matsubara, M., Katayose, S. & Maruoka, S. (2003) *Eur. J. Endocrinol.* **148,** 343–350.
36. Yamauchi, T., Kamon, J., Ito, Y., Tsuchida, A., Yokomizo, T., Kita, S., Sugiyama, T., Miyagishi, M., Hara, K., Tsunoda, M., *et al.* (2003) *Nature* **423,** 762–769.
37. Austin, B. P., Garthwaite, T. L., Hagen, T. C., Stevens, J. O. & Menahan, L. A. (1984) *Exp. Gerontol.* **19,** 121–132.
38. Yang, S. Q., Lin, H. Z., Mandal, A. K., Huang, J. & Diehl, A. M. (2001) *Hepatology* **34,** 694–706.
39. Shimomura, I., Hammer, R. E., Richardson, J. A., Ikemoto, S., Bashmakov, Y., Goldstein, J. L. & Brown, M. S. (1998) *Genes Dev.* **12,** 3182–3194.
40. Bluher, M., Michael, M. D., Peroni, O. D., Ueki, K., Carter, N., Kahn, B. B. & Kahn, C. R. (2002) *Dev. Cell* **3,** 25–38.
41. Chanussot, F., Ulmer, M., Ratanasavanh, R., Max, J. P. & Debry, G. (1984) *Int. J. Obes.* **8,** 259–270.
42. Clark, J. M. & Diehl, A. M. (2002) *Curr. Diab. Rep.* **2,** 210–215.
43. Petersen, K. F., Oral, E. A., Dufour, S., Befroy, D., Ariyan, C., Yu, C., Cline, G. W., DePaoli, A. M., Taylor, S. I., Gorden, P. & Shulman, G. I. (2002) *J. Clin. Invest.* **109,** 1345–1350.
44. Kraegen, E. W., Clark, P. W., Jenkins, A. B., Daley, E. A., Chisholm, D. J. & Storlien, L. H. (1991) *Diabetes* **40,** 1397–1403.
45. Goetze, S., Bungenstock, A., Czupalla, C., Eilers, F., Stawowy, P., Kintscher, U., Spencer-Hansch, C., Graf, K., Nurnberg, B., Law, R. E., *et al.* (2002) *Hypertension* **40,** 748–754.
46. Carvalheira, J. B., Ribeiro, E. B., Folli, F., Velloso, L. A. & Saad, M. J. (2003) *Biol. Chem. Hoppe-Seyler* **384,** 151–159.
47. Bruning, J. C., Gautam, D., Burks, D. J., Gillette, J., Schubert, M., Orban, P. C., Klein, R., Krone, W., Muller-Wieland, D. & Kahn, C. R. (2000) *Science* **289,** 2122–2125.
48. Guo, S., Rena, G., Cichy, S., He, X., Cohen, P. & Unterman, T. (1999) *J. Biol. Chem.* **274,** 17184–17192.
49. Zabolotny, J. M., Bence-Hanulec, K. K., Stricker-Krongrad, A., Haj, F., Wang, Y., Minokoshi, Y., Kim, Y. B., Elmquist, J. K., Tartaglia, L. A., Kahn, B. B. & Neel, B. G. (2002) *Dev. Cell* **2,** 489–495.
50. Kim, J. K., Zisman, A., Fillmore, J. J., Peroni, O. D., Kotani, K., Perret, P., Zong, H., Dong, J., Kahn, C. R., Kahn, B. B. & Shulman, G. I. (2001) *J. Clin. Invest.* **108,** 153–160.